URSI GASS 2021, Rome, Italy, 28 August - 4 September 2021

Numerical and experimental evaluation of Radiohelmet-to-UAV LoRa Links

Giulio M. Bianco*[(1,2)], Abraham Mejia-Aguilar[(2)], and Gaetano Marrocco[(1)]
(1) Pervasive Electromagnetics Lab, University of Rome Tor Vergata, Rome, Italy
(2) Center for Sensing Solutions, EURAC Research, Bolzano, Italy

Abstract

Body-worn radios exploiting the recently introduced LoRa protocol are very promising for Search and Rescue (SaR) operations in harsh environments. If the GPS signal is unavailable and there is not visual Line-of-Sight (LoS), the body-worn transmitting beacon could be localized based on the Received Signal Strength (RSS) measured by the rescuers. Moreover, an Unmanned Aerial Vehicle (UAV) equipped with a LoRa receiver could scout a vast area in little time and swiftly collect multiple RSS measurements. In this paper, the RSS seen by the UAV when a transmitting LoRa beacon is embedded in a safety helmet is evaluated through a two-ray model. The numerical values are corroborated using a flying UAV with good agreement.

1 Introduction

Recently introduced Low-Power Wide-Area Networks (LPWANs) allow covering kilometric communication ranges while keeping low power consumption and are very promising for creating a new generation of wearable devices. Radiofrequency beacons exploiting the LoRa LPWAN protocol are currently under study for mountain Search and Rescue (SaR) operations [1, 2]. If the target of the search wears a LoRa beacon, rescuers can exploit the Received Signal Strength (RSS) of the transmitted emergency signal to localize the target through algorithms [3]. Classical RSS-based localization algorithms use the monotonic proportionality between the RSS and the transmitter-receiver distance, even if the actual propagation environment is unknown [4]. So far, only terrestrial links have been considered. However, mountain SaR operations usually take places in extremely harsh terrains, wherein the time required to collect the measurements can be high, while the survival chances of the target could drop very quickly, especially in case of avalanches [5]. Unmanned Aerial Vehicles (UAVs) could search a vast area in little time while collecting many RSS measurements to speed up the localization.

In this paper, we address for the first time the body-to-UAV link through numerical and experimental analysis. An approximated expression of the antennas' gains and the Flat Earth Two-Ray (FE2R) model, usually employed for ground-to-air channels [6], are used to predict the RSS seen by the UAV when taking into account also the radiation pattern of the directive receiving antenna. Lastly, we measure some RSS profiles and compare them with the predicted ones, to assess the accuracy of the FE2R model and analyze the effects of the UAV flying height.

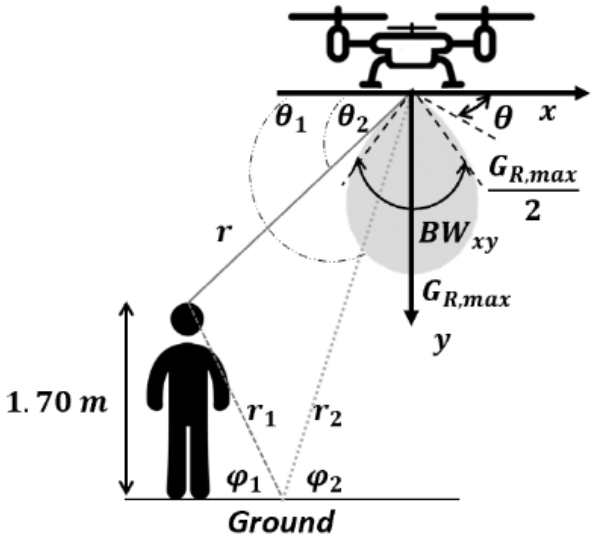

Figure 1. The FE2R model of the link. Since the earth is flat, $\varphi_1 = \varphi_2$. The gain G_R of the UAV-mounted circularly polarized patch was drawn by computing (4).

2 The numerical model of the ground-air link

The expected RSS seen by the drone P_R can be evaluated by resorting to the following link budget equation (in dB scale):

$$P_R = P_T + G_T + G_R + \chi - PL, \qquad (1)$$

where P_T is the transmission power, G_T and G_R are respectively the gain of the transmitting and the receiving antennas, χ is the polarization loss factor, and PL is the Path Loss [3]. The antennas' impedances are assumed perfectly matched.

The FE2R model accounts for the two-ray interference by adding to the right term of (1) the path-gain factor F [7]

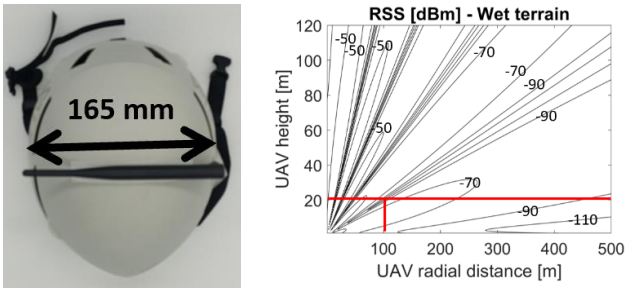

(a) (b)

Figure 2. a) The radiohelmet prototype. The wearable helmet antenna is a dipole fixed along the coronal plane. b) Numerically evaluated RSS in case of wet terrain. For flying heights lower than 20 m and radial distances longer than 100 m, the RSS monotonically decreases when the radiohelmet-UAV distance increases.

$$F = 20\log_{10}\left[\left|1 + \rho e^{-j\psi}\Gamma(\boldsymbol{\theta})e^{-jk_0(r-r_1-r_2)}\right|\right]$$
$$\Gamma(\boldsymbol{\theta}) = \sqrt{\frac{G_T(\theta_1')G_R(\theta_1)}{G_T(\theta_2')G_R(\theta_2)}} \quad (2)$$

where $\rho e^{-j\psi}$ is the Fresnel reflection coefficient of the ground, k_o is the propagation constant, gains are in the linear scale, r and $\boldsymbol{\theta} = [\theta_1, \theta_2, \theta_1', \theta_2']$ are respectively the path of the rays and the corresponding directions' vector according to Fig. 1. When considering an incident wave polarized parallelly to the ground, the Fresnel reflection coefficient reduces to [7]

$$\rho e^{-j\psi} = \frac{\sin\varphi - \sqrt{\frac{\varepsilon}{\varepsilon_0} - \cos^2\varphi}}{\sin\varphi + \sqrt{\frac{\varepsilon}{\varepsilon_0} - \cos^2\varphi}} \quad (3)$$

ε_0 being the vacuum permittivity, ε the complex dielectric permittivity of the terrain and φ the angle of incidence of the wave on the ground. Values of ε depend on both the composition and wetness of the ground. A wet terrain can be at the limit approximated with a perfect electric conductive plane having $\rho e^{-j\psi} = -1$ whereas a typical ε value for extremely dry terrains is $\varepsilon = \varepsilon_0(4.8 - 0.4j)$ [8]. Any terrain is expected to have a complex permittivity comprised between these two boundary conditions.

The considered transmitting antenna of the radiohelmet (i.e. the helmet embedding the LoRa radio) is a dipole

Table 1. Values considered to evaluate the RSS.

Parameter	Considered value
P_T	14 dBm
G_T	-2.1 dBi
$G_{R,max}$	3.2 dBi
$BW_{\xi y}$	1.745 rad

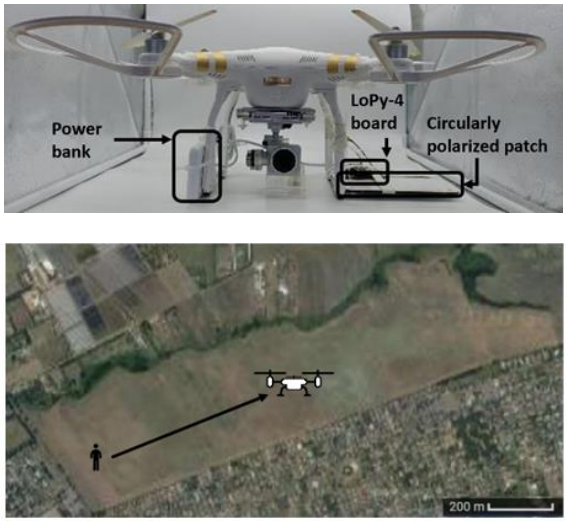

(a) (b)

Figure 3. (a) The UAV equipped with a LoRa receiver. (b) Satellite image of the uncultivated field selected for the measurements and the flight path of the UAV.

placed on the safety helmet's coronal plane (Fig. 2.a; commercial dipole from [9]). The receiver is mounted on a UAV, and it is connected to a circularly polarized patch. G_T is assumed constant for all directions and equal to the median value of $G_T(\theta')$ in all directions θ', evaluated through numerical simulations comprising a homogeneous head phantom ($\varepsilon = 42.7, \sigma = 0.99$ S/m [10]). The receiving antenna is parametrized by knowing its maximum gain $G_{R,max}$ and its beamwidth $BW_{\xi y}$ [11]:

$$G_R(\theta) = G_{R,max}\left[\frac{f(BW_{\xi y})\sin\theta}{(\cos\theta)^2 + f(BW_{\xi y})(\sin\theta)^2}\right]^2$$
$$f(BW_{\xi y}) = \tan\left(\frac{BW_{\xi y}}{2}\right)\frac{\sin\left(\frac{BW_{\xi y}}{2}\right)}{\sqrt{2} - \cos\left(\frac{BW_{\xi y}}{2}\right)} \quad (4)$$

where the origin is on the patch, angles are in radians, $0 < \theta < \pi$, the gain is expressed in linear scale, and ξ identifies both the *x*- and the *z*-axis (w.r.t. Fig. 1). Lastly, the considered PL is the free-space PL for 868 MHz signals, which is the centre-band frequency of the European LoRa 863-873 MHz band.

Tab. 1 reports the electromagnetic parameters we inserted in (1) and (4) to evaluate the RSS seen by the UAV. The numerically evaluated RSS in case of wet terrain for a low-altitude UAV and a maximum radial distance of 500 m is shown in Fig. 2.b. The RSS monotonically decreases when the distance increases for a flying height lower than 20 m and a helmet-UAV distance longer than 100 m. For flying heights higher than 90 m, the RSS is not proportional to the radial distance even for distances longer than 500 m, and, therefore, such RSS profiles can hardly be used for localization purposes, unless ad-hoc algorithms are employed.

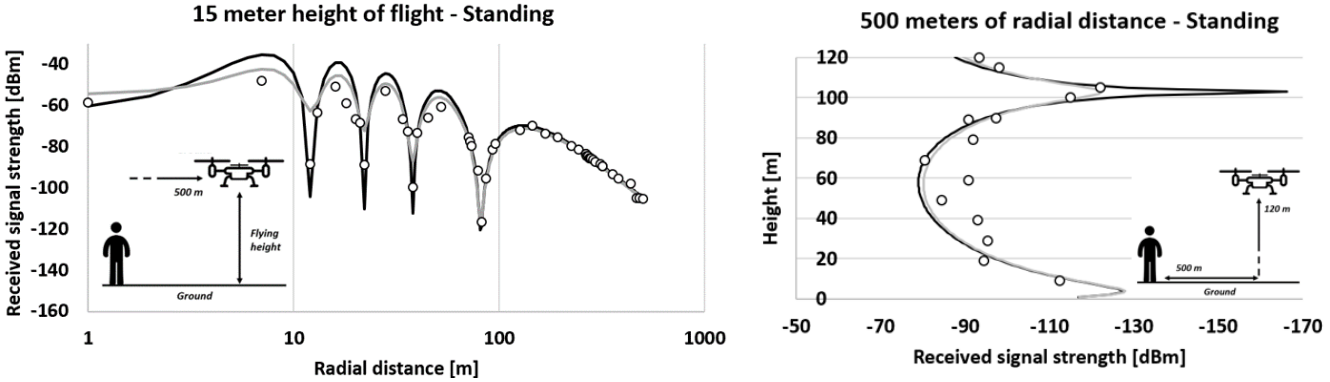

(a) (b)

Figure 4. Theoretical (lines) and measured (circles) RSS seen by a UAV when the radiohelmet transmits. The uncertainty on the terrain's wetness is accounted for by the two boundary conditions of wet terrain (black line) and extremely dry terrain (grey line) as specified in Sec. 2. The insets describe (a) the horizontal flight and (b) the vertical flight.

3 RSS measurements

A volunteer (1.70 m tall, as in the simulations) wore the radiohelmet prototype embedding a LoPy-4 board broadcasting LoRa packets (transmission parameters as in [3]). The LoRa receiver comprised a LoPy-4 board and a Keonn Advantenna p-11 patch, whose maximum gain and beamwidth (from datasheet) are equal to those in Tab. 1. The receiver was installed on DJI Phantom 3 Pro UAV (Fig. 3.a). The UAV flew over an uncultivated field near Colle Romito (Ardea, Italy; Fig. 3.b). The weather was sunny during the flights, which were performed in September 2020. There were no obstacles so that the receiver was in Line-of-Sight (LoS) condition, and bushes covered the terrain. The UAV's flight speed was kept lower than 1 m/s to avoid any Doppler effect. The RSS was estimated by the Received Signal Strength Indicator and the Signal-to-Noise ratio [3]. The RSS estimation was improved by introducing a single-point calibration [12] through a spectrum analyzer (Anritsu MS2711A)

Fig. 4 shows the measured RSS values compared with the simulated ones during the horizontal flight (Fig. 4.a) and the vertical flight (Fig. 4.b). In Fig. 4.a it is possible to see that the RSS is monotonical for radial distances longer than 100 m, as correctly predicted by the model (Fig. 2.b). In average, the simulations overestimate the measured RSS of about 5 dB. Differences are mostly due to the simplified antennas' models. The error is higher for radial distances shorter than 100 m because of the heavy two-ray interference. Overall, numerical and experimental results are in good agreement. Despite its simplicity, the model was suitable to predict the complex interference patterns for both horizontal and vertical flights of the UAV.

4 Conclusions

We evaluated the expected RSS by a patch-equipped UAV when a helmet embedding a LoRa radio is transmitting. We compared the expected values returned by the FE2R model with the measured ones with reasonable agreement. The results demonstrate that the two-ray interference can be mitigated by keeping the flying height of the UAV lower than 20 m so to maintain the RSS directly proportional to the radiohelmet-UAV distance for radial distances longer than 100 m. The monotonical RSS allows for the localization of the target through classical RSS-based localization algorithms. Further tests revolving a fallen target will be shown at the conference. We will show that a fully monotonic link is established when the user is lying on the ground

5 Acknowledgements

The research leading to these results has received funding from the European Regional Development Fund under the Cooperation Programme Interreg V-A Italia Austria 2014-2020, ITAT3023, Smart Test for Alpine Rescue Technology START, and from H2020-MSCA-RISE funding under the project HERCULES (Nr. 778360).

6 References

1. G. M. Bianco, A. Mejia-Aguilar and G. Marrocco, "Performance evaluation of LoRa LPWAN technology for mountain search and rescue," in *Proc. 5th Int. Conf. Smart Sustain. Technol.*, Split, Croatia, Sept. 23-26 2020, pp. 1-4.

2. G. M. Bianco, A. Mejia-Aguilar and G. Marrocco, "Radio wave propagation of LoRa systems in mountains for search and rescue operations," in *Proc. 23rd General*

Assem. Scientific Symp. Int. Union Radio Sci., Rome, Italy, Aug. 29 - Sept. 5 2020, pp. 1-3.

3. G. M. Bianco, R. Giuliano, G. Marrocco, F. Mazzenga and A. Mejia-Aguilar, "LoRa system for search and rescue: path-loss models and procedures in mountain scenarios," in *IEEE Internet of Things J.*, **8**, no. 3, pp. 1985-1999, Feb. 2021.

4. X. Li, "Rss-based location estimation with unknown pathloss model," *IEEE Trans. Wireless Commun.*, **5**, no. 12, pp. 3626–3633, Dec. 2006.

5. V. Ferrara, "Technical survey about available technologies for detecting buried people under rubble or avalanches," in *Disaster Management and Human Health Risk IV*, *1*st edition, Southampton, UK; Wit Press, 2015, ch. 3, pp. 91-101.

6. A. A. Khuwaja, Y. Chen, N. Zhao, M. Alouini and P. Dobbins, "A survey of channel modeling for UAV communications," *IEEE Commun. Surv. Tut.*, **20**, no. 4, pp. 2804-2821, doi: 10.1109/COMST.2018.2856587.

7. R. E. Collin, "Radio-wave propagation", in *Antennas and Radiowave Propagation*, New York, NY, USA, Mc-Graw Hill, 1985, ch. 6, sec. 1, pp. 339-349.

8. *P.527: Electrical characteristics of the surface of the Earth*, ITU-R P.527-4, June 2017. [Online]. Available: https://www.itu.int/rec/R-REC-P.527-4-201706-I/en

9. *LoRa (868MHz/915MHz) & Sigfox Antenna Kit*, Pycom Company, Guildford, U.K., 2017. Accessed: Feb. 10, 2021. [Online]. Available: https://pycom.io/product/lora-868mhz-915mhz-sigfox-antenna-kit/

10. *IEEE Recommended Practice for Determining the Peak Spatial-Average Specific Absorption Rate (SAR) in the Human Head from Wireless Communications Devices: Measurement Techniques*, IEEE 1528-2013, IEEE Standards Association, Sept. 2013. [Online]. Available: https://standards.ieee.org/standard/1528-2013.html

11. G. Marrocco, E. Di Giampaolo and R. Aliberti, "Estimation of UHF RFID reading regions in real environments," *IEEE Antennas Propag. Mag.*, **51**, no. 6, pp. 44-57, Dec. 2009

12. *SX1272/73 Datasheet*, Semtech Corporation, Camarillo, CA, USA, 2017. Accessed: Mar. 24, 2020. [Online]. Available: https://www.mouser.com/datasheet/2/761/sx12721277619.pdf